Advanced diffusion studies with isotopically controlled materials

Hartmut A. Bracht[a], Hughes H. Silvestri[b] and Eugene E. Haller[b,] *

[a]Institut für Materialphysik, Universität Münster, Germany.
[b]Department of Materials Science and Engineering, University of California Berkeley, and Lawrence Berkeley National Laboratory, Berkeley, CA, 94720.

Keywords: self-diffusion, foreign atom diffusion, semiconductors, point defects, stable isotopes, SIMS
PACS: 66.30.Hs, 66.30.Jt, 61.72.Ji, 82.20.Tr

Abstract

The use of enriched stable isotopes combined with modern epitaxial deposition and depth profiling techniques enables the preparation of material heterostructures, highly appropriate for self- and foreign-atom diffusion experiments. Over the past decade we have performed diffusion studies with isotopically enriched elemental and compound semiconductors. In the present paper we highlight our recent results and demonstrate that the use of isotopically enriched materials ushered in a new era in the study of diffusion in solids which yields greater insight into the properties of native defects and their roles in diffusion. Our approach of studying atomic diffusion is not limited to semiconductors and can be applied also to other material systems. Current areas of our research concern the diffusion in the silicon-germanium alloys and glassy materials such as silicon dioxide and ion conducting silicate glasses.

* corresponding author

Introduction

The diffusion of atoms in materials is a fundamental process of mass transport that is important for numerous applications. For example, doping of silicon is often performed by the diffusion of the desired foreign-atom into the material. The current standard of very shallow dopant profiles of only a few tenths of nanometers by ion implantation requires a strong control of diffusion and reaction processes in order to minimize transient-diffusion effects [1]. With the down-scaling of Si-based electronic devices, interfaces are becoming more significant and can affect the diffusion in the bulk material of interest. In this context, the reactions occurring at the SiO_2/Si interface are very important in order to understand the oxidation process of Si and the ability of the interface to act as a source of point defects. The large scale production of electronic and optoelectronic devices based on group III-V compound semiconductors also requires highly reproducible doping processes. To meet this requirement the reason for the often observed complicated shape of dopant profiles in compound semiconductors must be understood. These examples illustrate that a comprehensive understanding of the mechanisms of dopant diffusion and the properties of native point defects in the underlying material, which includes their generation, recombination and interaction with dopant atoms, are of fundamental significance for controlling the fabrication of electronic devices.

Numerous studies on diffusion in semiconductors have been performed over the last five decades and published in scientific journals. Unfortunately, the earliest diffusion studies are not cited in electronic databases although some of the earlier results are of fundamental significance and still relevant for semiconductor technology. In order not to lose sight of the source of many fundamental results, sources other than electronic databases should be considered. In this context we point to the Landolt-Börnstein New Series, which comprise a comprehensive data collection on the diffusion, the solubility and electronic properties of point defects in semiconductors [2,3].

Information about the nature and properties of point defects in semiconductors can be obtained from spectroscopic methods such as electron paramagnetic resonance (EPR) studies, infrared (IR) spectroscopy, deep level transient spectroscopy (DLTS) and perturbed angular correlation (PAC) experiments, to name just a few. All of these methods provide information about the properties of defects at temperatures which range from cryogenic to room temperature. However a generally applicable spectroscopic method for studying point defects at temperatures relevant for process technology is not available. An exception is the positron annihilation spectroscopy (PAS). But this method is limited to the investigation of vacancy-like defects and unfortunately even fails in the case of silicon because the concentration of vacancies in thermal equilibrium is below the detection limit of the method. On the other hand, theoretical calculations of the structure and formation energy of point defects in solids are very valuable for comparison with spectroscopic results. But it remains unclear how far these theoretical results, obtained for zero Kelvin, are applicable at higher temperatures. The numerous theoretical papers published on point defects and more complex defect structures in solids reflect the need to gain information about the properties of the defects which strongly affect the functionality of technological materials.

A general method to investigate the nature and properties of point defects in materials at high temperatures is “diffusion spectroscopy”. On first sight this appears to be an oxymoron but diffusion studies can in fact be performed in such a way that detailed information about point defects become accessible. This advance in solid state diffusion is highlighted by the present contribution which summarizes our recent developments and results on self- and foreign-atom diffusion in semiconductors. For diffusion spectroscopy, we utilized appropriate isotopically controlled heterostructures which enable diffusion experiments over a wide temperature range. We performed self-diffusion experiments under thermal equilibrium and radiation enhanced conditions. Finally, by means of isotope heterostructures the impact of dopant diffusion on self-diffusion could be investigated for the first time. Such experiments provide valuable information about the atomic mechanisms and properties of point defects that are not accessible by self- and foreign-atom diffusion experiments performed separately.

Self-diffusion in semiconductors under thermal equilibrium conditions

Common studies of self-diffusion in solids use either enriched stable or radioactive isotopes as tracer elements that are deposited on top of the material of interest. After diffusion anneals, the penetration profiles of the tracer are measured by depth profiling techniques and instruments to detect the specific isotopic mass or the radioactivity. Self-diffusion experiments performed in this way are restricted to the natural abundance of the stable isotope in the material

or by the limited half-life of the radiotracer. Moreover, the diffusion of the tracer from the surface into the bulk material can be affected by surface layers caused, for example, from exposure to air. With enriched stable isotopes and modern epitaxial deposition techniques such as molecular beam epitaxy (MBE) or chemical vapor deposition (CVD), isotopically enriched epitaxial layers can be grown. An appropriate layer structure for self-diffusion experiments consists of an isotopically enriched layer sandwiched between two layers of the same material with natural composition. The thickness of the isotope layer should be sufficient to enable diffusion experiments over a wide range of temperatures. The use of buried isotopically enriched layer structures for self-diffusion studies avoids any limitations that may be caused by the half-live of radioactive tracers and/or by effects originating at surfaces.

Self-diffusion in Ge

The first experiments that demonstrated the benefits of stable isotopes for diffusion experiments were realized with the MBE growth of germanium isotopic heterostructures [4]. Growing epitaxial layers of enriched ^{70}Ge and ^{74}Ge on a Ge substrate of natural isotopic abundance allowed for the observation of Ge self-diffusion at a buried interface [4]. Figure 1 illustrates the depth profiles of all 5 stable Ge isotopes measured by means of secondary ion mass spectrometry after annealing of the isotope structure. Fitting of the solutions of Fick's law of self-diffusion, i.e., complementary error functions, to the experimental Ge profiles yields the Ge self-diffusion coefficient. The good agreement with self-diffusion data obtained from traditional diffusion studies that utilized the radioactive ^{71}Ge tracer isotope [5] demonstrates the usefulness of isotope structures for self-diffusion experiments. Further results which include the impact of doping and hydrostatic pressure on Ge self-diffusion [5] and the vacancy contribution to Ge diffusion determined from the dissociative diffusion of Cu in Ge clearly demonstrate that self-diffusion in Ge is mainly controlled by vacancies [6,7] with an activation enthalpy of 3.09 eV [5].

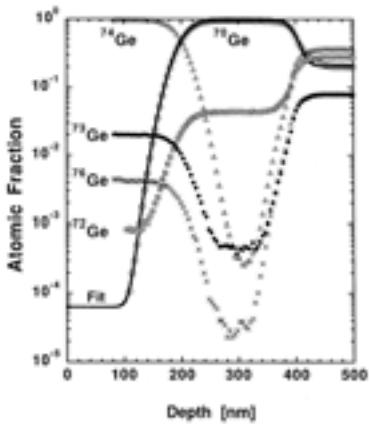

Figure 1 SIMS depth profiles of the Ge isotope heterostructure after annealing at 586 °C for 55.55 h. The depth profiles of the stable isotopes ^{70}Ge, ^{72}Ge, ^{73}Ge, ^{74}Ge and ^{76}Ge are given as a function of atomic fraction. The fit to the ^{70}Ge profile is shown. [4]

Self-diffusion in Si

Previous Si self-diffusion experiments were performed with radioactive and stable isotopes in conjunction with various depth profiling methods (see e.g. Ref. [2]). All methods

provided self-diffusion data only for a limited temperature range. Self-diffusion data determined for temperatures above and below 1300 K suggested an activation enthalpy of about 5 eV and 4 eV, respectively. Hence a kink in the temperature dependence of Si self-diffusion was proposed which reflects the change from a self-interstitial mediated self-diffusion at high temperatures to a vacancy-mediated self-diffusion process at lower temperatures. A major limitation of the previous self-diffusion studies was related to the short half-life of the Si radioactive isotope, ^{31}Si, ($t_{1/2}$ = 2.6 h). As a result, diffusion studies with ^{31}Si were limited to high temperatures such that within the time window for the experiment a measurable diffusion of the radiotracer into the sample was still observed. With the use of ^{28}Si enriched epitaxial layers grown on a natural Si substrate this limitation was overcome and we could investigate Si self-diffusion over a wide temperature range (855 to 1388 °C) [8]. Typical Si profiles measured with SIMS after annealing an isotope structure with a ^{28}Si epitaxial layer grown on natural Si are illustrated on the left side of Figure 2. The temperature dependence of the Si self-diffusion coefficient is accurately described over seven orders of magnitude with one diffusion activation enthalpy of 4.76 eV [8,9]. This shows that there is no pronounced kink in the temperature dependence of Si self-diffusion. However, this does not imply that only one mechanism mediates self-diffusion but rather that one mechanism predominates in the temperature range investigated.

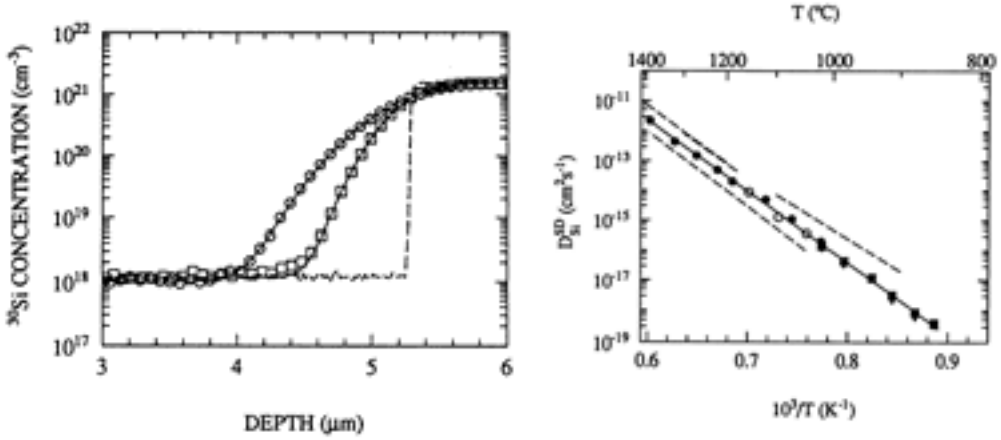

Figure 2 (left) SIMS depth profiles of ^{30}Si in a structure consisting of a ^{28}Si enriched epitaxial layer grown on a substrate of natural composition. Profiles were obtained after diffusion annealing at 1095 °C for 54.5 h (squares) and 1153 °C for 19.5 h (circles) [8]. The dashed line is the as grown ^{30}Si profile. (right) An Arrhenius plot of the self-diffusion coefficient of Si which shows the experimental data (symbols) and the Arrhenius-type temperature dependence of our results (solid line) compared to results given in the literature (taken from [8]).

Comparison of the self-diffusion data with the individual contributions of self-interstitials and vacancies to Si diffusion, which were obtained from Zn-diffusion experiments [10,11,12,13], demonstrate that Si diffusion is mainly mediated by self-interstitials in the temperature range investigated. Relative to the interstitial contribution to self-diffusion, the contribution of vacancies increases with decreasing temperature and approaches the interstitial contribution at temperatures below 1200 K. The individual contributions to Si self-diffusion can be further separated into the contributions of the existing charge states of the native defects. This was

achieved by the simultaneous analysis of self- and dopant diffusion in isotope multilayer structures, which is summarized in a later section.

Self-diffusion in group III-V compound semiconductors

Self-diffusion in binary compound semiconductors is more complex compared to elemental semiconductors due to the higher number of possible native point defects that can, in principle, mediate self-diffusion. In addition to vacancies and self-interstitials on the corresponding sublattices, antisite defects must be considered. Using highly enriched ^{69}Ga and ^{71}Ga materials the diffusion of Ga in Ga-based III-V compounds was investigated. Figure 3 shows depth profiles of ^{69}Ga and ^{71}Ga in ^{71}GaAs/^{69}GaAs [14] and ^{71}GaP/^{69}GaP [15] along with the Arrhenius plot of the Ga self-diffusion coefficients for both materials. In addition, we studied the Ga self-diffusion and Al-Ga interdiffusion by means of $Al_x{}^{71}Ga_{1-x}As/Al_y{}^{69}Ga_{1-y}As/^{71}GaAs$ isotope heterostructures grown on natural GaAs [16]. By monitoring the diffusion of ^{69}Ga and ^{71}Ga at the AlGaAs/AlGaAs interface with SIMS, the Ga diffusion was found to decrease with increasing Al content. The intermixing observed at the AlGaAs/GaAs interface can be accurately described with a concentration-dependent interdiffusion coefficient. The activation enthalpy determined for Ga diffusion in $Al_xGa_{1-x}As$ remained constant at 3.6±0.1 eV for x between 0 and 1.0 while the pre-exponential factor decreased with increasing Al concentration. The lower Ga diffusivity in AlAs compared to GaAs reflects a lower thermal equilibrium concentration of vacancies in AlAs as compared to GaAs. Different equilibrium values of group III vacancies in AlAs and GaAs can be explained with the difference in the electronic structure between these materials. Compared to Ga diffusion in GaAs a higher Al diffusivity was observed in AlGaAs, which is consistent with the higher jump frequency of ^{27}Al compared to ^{71}Ga, due to the differences in their masses. Finally, we also investigated the effect of n- and p-type doping on the diffusion of ^{69}Ga at a ^{71}GaAs/$^{nat.}$GaAs isotope structure [17]. This work provides strong evidence that Ga self-diffusion in GaAs is controlled by Ga vacancies that can exist in either its neutral, or in its singly or doubly negative charge state. The relative contributions of the various charged vacancies to Ga diffusion vary with temperature and doping. A major contribution of triply negatively charged vacancies, whose existence was predicted from total energy calculations [18] and which were proposed to control Ga diffusion under intrinsic and n-type doping conditions [19], was not found.

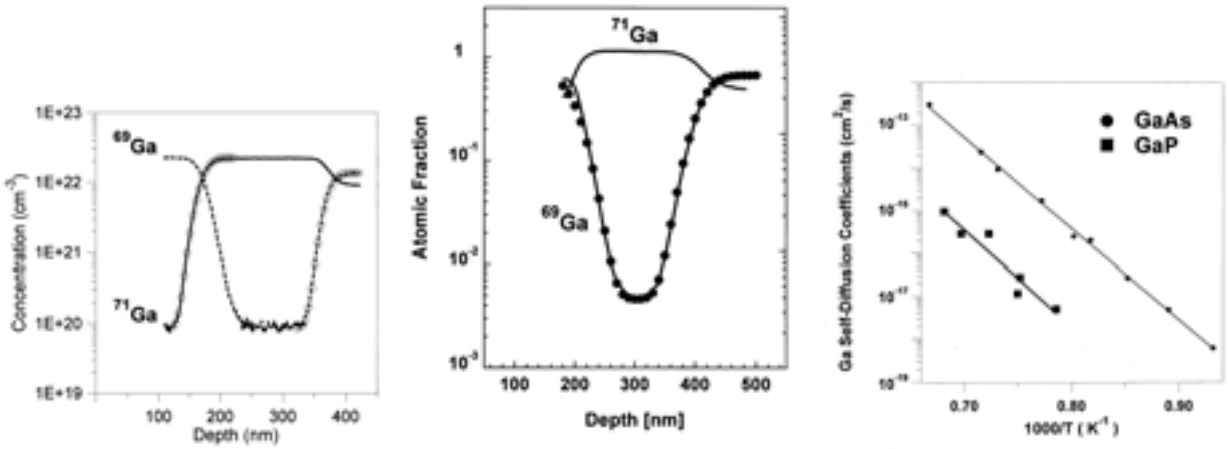

Figure 3 SIMS depth profiles of ^{69}Ga and ^{71}Ga in GaAs (left) and GaP (middle) isotope epilayers

(circles are theoretical fits). The GaAs sample was annealed at 974 °C for 3321 s [14] while the GaP sample was annealed at 1111 °C for 231 min [15]. (right) Arrhenius plot of Ga self-diffusion in GaAs (circles) and GaP (squares) [15].

Since both As and P are mono isotopic elements, the self-diffusion of these group-V elements can not be investigated with isotope heterostructures. In this case, diffusion experiments can only be performed with radioactive isotopes of As and P either deposited on top of the surface or implanted into the material of interest [20]. In contrast to the elements As and P, two stable isotopes exist for antimony (^{121}Sb and ^{123}Sb). With ^{69}Ga^{121}Sb/^{71}Ga^{123}Sb isotope heterostructures we studied the diffusion of Ga and Sb simultaneously. Earlier experiments on Ga and Sb diffusion in GaSb, which were performed with radioactive isotopes, revealed similar results for the Ga and Sb diffusivity [21]. These results were explained with a coupled diffusion mechanism that involves a defect formed by two Ga vacancies and one Ga anti-site atom [21]. Our result clearly demonstrated that Ga and Sb diffuse independently [22,23], i.e., on their own sublattice, and hence disproved the earlier proposed so-called triple defect mechanism. The large difference between Ga and Sb diffusion is evident in Figure 4. Compared to the as-grown structure (Fig. 4(a)), annealing at 700°C for 1005 min leads to a pronounced broadening of the Ga sublattice whereas the Sb sublattice remains unaffected. After annealing for about 18 days at 700°C a small intermixing on the Sb sublattice was observed while the Ga isotopes had reached a homogenous distribution. Very low Sb diffusion coefficients of 10^{-18} cm^2s^{-1} even at temperatures close to the melting point were measured. This has never been observed for any other solid [22]. This unusual result was explained with exceptionally low concentrations of Sb vacancies and Sb interstitials resulting from transformations among native point defects [22].

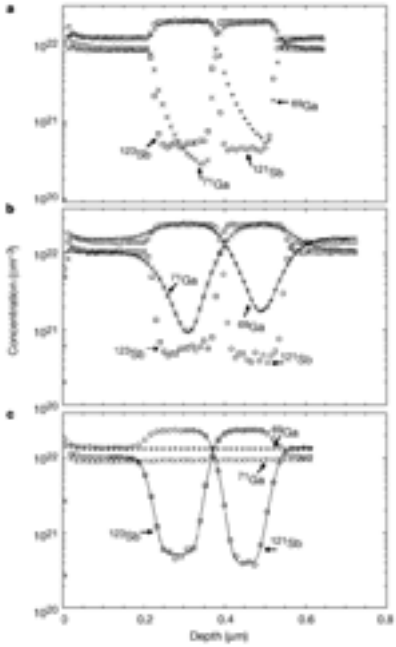

Figure 4 SIMS depth profiles of ^{69}Ga^{121}Sb/^{71}Ga^{123}Sb isotope heterostructures. a) As grown b) After anneal under Sb-rich conditions at 700 °C for 105 min and 18 days (c). [22]

In order to clarify the mechanisms of self-diffusion in group III-V compound semiconductors, a comparison of the total self-diffusion coefficient with the individual contributions of native point defects to self-diffusion is required. Such contributions can be obtained from modeling of dopant diffusion. The diffusion of Zn in GaSb provides strong evidence that Ga diffusion in GaSb under Ga-rich conditions is mainly mediated by neutral Ga interstitials [24]. Zn diffusion in GaP also seems to indicate that neutral Ga interstitials mediate Ga diffusion [25,26] but still further investigations are required. Recent results on Ga and Zn diffusion in GaAs [17,27,28] are consistently explained with a Ga vacancy-mediated Ga diffusion under standard conditions (electronically intrinsic conditions and an arsenic partial pressure of 1 atm) and the existence of neutral and singly positively charged Ga interstitials whose contribution to Ga diffusion lies below the total Ga diffusion coefficient.

In addition to self-diffusion in group III-V compound semiconductors, we also investigated the self-diffusion of Si and C by means of isotopically enriched $^{28}Si^{12}C$ epitaxial layers grown on natural SiC [29]. The experiments show that the diffusion of Si and C is of the same order of magnitude but several orders of magnitude lower than earlier self-diffusion data reported in the literature [30,31]. From the observed interrelation between self- and B-diffusion in SiC we concluded that C diffusion is mediated by C interstitials. The defect mediating Si diffusion is still unknown but it is likely that both Si vacancies and interstitials contribute with a preference for either species depending on the doping level.

Interference between self-atom and dopant diffusion

Isotopically controlled heterostructures are well suited to investigate the impact of dopant diffusion on self-diffusion. For these experiments we used isotope multilayer structures that allow the measurement of depth-dependent self-diffusion, which results from the diffusion of a dopant into the isotope structure. The incorporation of dopants to concentrations that exceed the intrinsic carrier concentrations makes the material extrinsic. As a consequence, the position of the Fermi level shifts, leading to a change in the thermal equilibrium concentration of charged native defects [32]. Accurate modeling of the simultaneous diffusion of self- and dopant atoms not only provides a greater insight into the mechanisms of diffusion but also about the properties of the point defects involved. These properties include the nature of the point defects, their charges states and their contributions to self-diffusion.

Zn diffusion experiments in a GaAs isotope structure consisting of 10 pairs of $^{69}GaAs/^{71}GaAs$ layers were performed to study impurity-induced layer disordering in group III-V compound semiconductors which was discovered by Laidig et al [33]. Zn and Ga diffusion profiles were simultaneously recorded by means of secondary ion mass spectrometry and accurately described assuming that neutral Ga interstitials and neutral and singly positively charged Ga vacancies are involved in Zn diffusion [27]. The Ga and Zn SIMS depth profiles and the computer model fits are presented in Figure 5. On the basis of this interpretation the observed near surface kink of the Zn profile is a consequence of a Ga vacancy-controlled Zn diffusion. The profile tail is formed by the diffusion of the neutral Ga interstitial. Since the underlying Zn diffusion model predicts contributions of Ga vacancies to Ga diffusion that exceed the total Ga diffusion coefficient, the mechanism of Zn diffusion in GaAs could not yet be determined precisely. New experiments confirmed the participation of neutral and also of singly positive Ga interstitials [28] and hence disproved the generally accepted interpretation of Zn diffusion in GaAs via doubly and triply positively charged Ga interstitials [34]. Additional

investigations are being performed currently to clarify the origin of the kink part of Zn kink-and-tail concentration profiles.

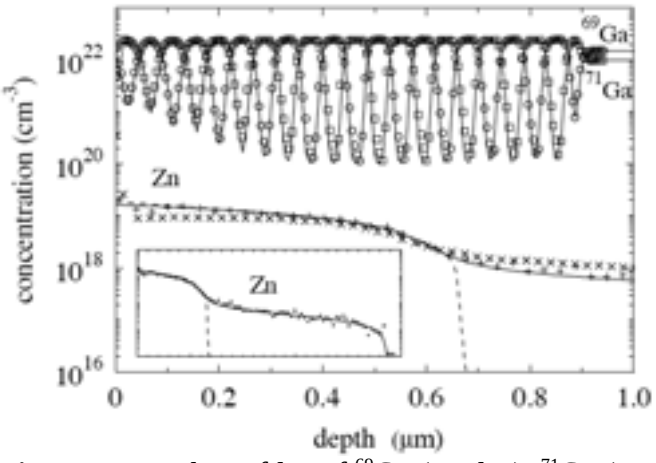

Figure 5 Depth profiles of ^{69}Ga (circles); ^{71}Ga (squares); and Zn (+) measured with SIMS after diffusion of Zn in a GaAs isotope heterostructure at 666 °C for 180 min. The concentration of electrically active Zn (×) measured by means of ECV profiling is shown for comparison. The solid lines represent simulations of Zn and Ga diffusion. The inset shows the entire Zn profile with a penetration depth of about 2.3 mm [27].

Simultaneous dopant and self-diffusion experiments were performed in Si stable isotope heterostructures consisting of 5 alternating pairs of ^{28}Si/$^{nat.}$Si. The dopants were introduced via implantation into an amorphous Si cap layer, thereby preventing any implantation damage from altering the equilibrium native defect concentrations in the isotope structure. The dopants B [35,36], As [36,37,38], and P [39] were investigated to determine the native defects and defect charge states responsible for diffusion in Si under extrinsic p- (B) and n- (As, P) type conditions. For B, the simultaneous diffusion experiments yielded a kick-out type diffusion mechanism mediated by neutral and singly positively charged Si self-interstitials [35,36]. In the case of As diffusion under extrinsic conditions, the stable isotope experiments showed that the vacancy and interstitialcy mechanisms are mediated by the neutral vacancy and singly negatively charged self-interstitial [36,37,38]. A plot of the SIMS depth profiles of As and Si in the stable isotope heterostructure, illustrating the capabilities of the simultaneous dopant and stable isotope diffusion technique, is given in Figure 6. In this figure three simulations for the three different charge states of the interstitial are plotted along with the As and Si depth profiles. It can be seen that the As profile is insensitive to the interstitial charge state. On the other hand the Si profile is highly sensitive, indicating the proper choice of defect charge state. The simultaneous diffusion of P and Si in the Si stable isotope heterostructure revealed that P diffusion is mediated by the neutral and singly negatively charged self-interstitial [39]. These three experiments also yielded the contributions of the neutral, singly negatively, and singly positively charged self-interstitial to Si self-diffusion [38]. The Arrhenius plot of the temperature dependence of the interstitial contributions and their sum are presented in Figure 7. It can be seen that the sum of these defect contributions agrees well with the total Si self-diffusion determined from earlier work [8]. Previously, we assigned the contribution of the negatively charged native point defect to Si diffusion to the negatively charged vacancy [36,37]. However, the simultaneous P and Si

diffusion shows that this contribution is more likely due to the singly negatively charged self-interstitial [39]. The results shown in Figure 7 suggest that the total Si self-diffusion coefficient is given by the sum of the neutral and singly positively and negatively charged self-interstitials. A contribution of vacancies is not evident. This contribution is hidden in the contribution of the neutral interstitial. A final analysis of all dopant and Si profiles which is in progress is expected to uncover this vacancy contribution to Si diffusion.

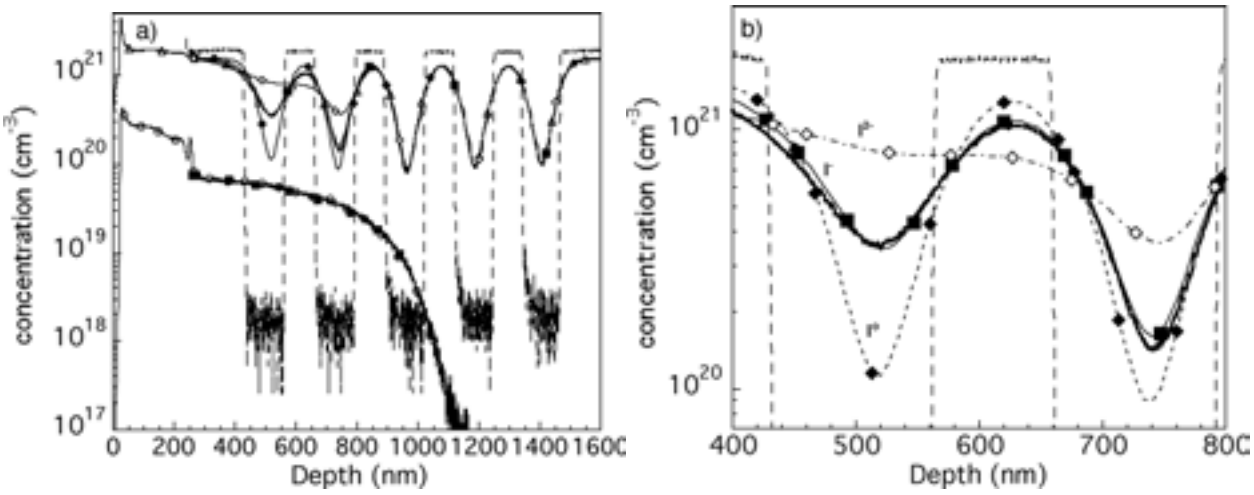

Figure 6 a) Concentration versus depth profile for an As implanted Si isotope heterostructure after annealing at 950 °C for 122 hours. Plot shows pre-anneal ^{30}Si profile (dashed line) along with the annealed profile. b) Enlarged view of the region of enhanced Si diffusion. Simulated diffusion profiles of different native defect charge states are included to show the variation of the simulation with the charge state. The singly negatively charged interstitial is shown to lead to the best fit to the data (solid line). [36,37,38]

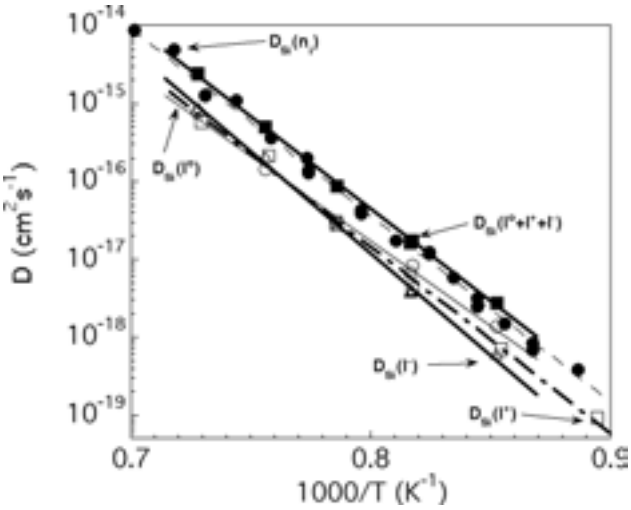

Figure 7 Plot of diffusion coefficient versus 1000/T for Si self-diffusion under intrinsic conditions [36,37,38]. The open symbols represent the individual contributions of native defects. The solid squares are the sum of the contributions of the native defects at each

temperature. The solid circles and thin dashed line represent the total self-diffusion values from [8] for comparison.

Radiation enhanced self-diffusion in silicon

Irradiation of isotope heterostructures with high energy particles such as protons or electrons creates native point defects in concentrations which significantly exceed the concentrations under thermal equilibrium conditions. As a consequence, radiation enhances self-diffusion. With isotope heterostructures, the radiation enhanced self-diffusion (RESD) can be investigated in a straightforward manner. In particular, isotope heterostructures enable the measurement of the depth dependence of RESD. A depth dependence is expected because during annealing and in situ radiation a steady state is established between the formation of native point defects and their annihilation by direct recombination and outdiffusion to the sample surface. The depth dependent RESD reflects the distribution of the native point defects in steady state. The distribution in steady state depends on the properties of the native point defects such as their thermal equilibrium concentration and diffusion coefficient. Detailed modeling of RESD provided direct evidence that vacancies in Si at high temperature diffuse more slowly than expected from their diffusion at low temperatures [40]. We concluded that this result is a consequence of the microscopic structure of the vacancy whose entropy and enthalpy of migration increase with increasing temperature. The recent experiments demonstrate that RESD in conjunction with numerical simulations of the diffusion process is a very powerful approach to determine the thermodynamic properties of native point defects. In the past neither epitaxially grown isotope structures for RESD experiments were available nor detailed numerical analyses were possible due to the limited computer capacity. These limitations no longer exist and hence open up advanced studies on radiation enhanced diffusion in materials.

Stable isotope self-diffusion in other solids

Self-diffusion experiments with isotopically enriched heterostructures are in principle applicable for all material systems where at least two stable isotopes of the material of interest exist. With the advance in thin layer deposition techniques, suitable isotope structures can be grown which limit the consumption of the isotope material and the sample cost. Another area of interest in a detailed understanding of the self- and foreign-atom diffusion behavior is self- and dopant diffusion in Si-Ge alloys. Dopant diffusion in Ge is not well understood [41] and accurate diffusion data are very limited [2]. Dopant diffusion in Ge and SiGe isotope multilayer structures would significantly improve our understanding of the mechanisms of diffusion in Ge and SiGe alloys and how they change with alloy composition and strain. This information is important in particular for the integration of these materials in the next generation of electronic devices.

Silicon dioxide is another important technological material. Glasses, optical fibers, dielectric thin films in integrated electronic circuits are just a few of its applications. For controlling the functionality of the oxide during thermal processing, detailed information about the dynamic of the network forming components are highly desirable. The availability of isotopically enriched Si and modern deposition and depth profiling techniques opened up

systematic investigations on Si diffusion in amorphous SiO_2. Several recent publications have addressed this important topic [42,43,44].

Doping of silica with alkali and alkaline-earth oxides strongly affects the glass transistion temperature and thereby the dynamic of the network forming elements. In order to investigate the dynamics of silicon and oxygen in silicate glasses isotopically enriched materials are very beneficial. Isotopically enriched silicate glasses can be prepared by means of the sol-gel method utilizing tetraethylorthosilicate (TEOS: $^{28}Si(OC_2H_5)_4$) enriched with ^{28}Si. Recently we synthesized enriched TEOS from elemental ^{28}Si and prepared thin isotopically enriched $^{28}SiO_2$ layers on natural SiO_2. The samples were used to investigate the diffusion of silicon in sol-gel derived silica glasses [45]. With the same approach, isotopically enriched silicate glasses doped with alkali and alkaline-earth oxides on top of equivalently doped silicate bulk glasses can be prepared and studied.

Conclusion and Future Outlook

Self- and dopant diffusion experiments with isotopically controlled semiconductors provide new insights into the mechanisms of diffusion and the properties of the point defects involved, which can not be obtained by means of self- and dopant diffusion experiments performed separately. Modelling of the simultaneous self- and dopant diffusion is a challenging task since all results obtained for the native point defects must be mutually consistent. In this respect, a final analysis of all dopant and Si profiles in Si isotope multilayer is still required to accurately determine the individual contributions of the native point defects to Si self-diffusion. In the case of GaAs, the interference between dopant and Ga diffusion has put the general interpretation of Zn diffusion in GaAs into question. One aspect of this question concerns the origin of the Zn diffusion tail, which is now consistently explained by a neutral Ga interstitial mediated Zn diffusion [28]. Isotope structures are also very suitable to investigate the radiation enhancement of diffusion. Experiments on radiation enhanced self-diffusion of Si demonstrate the power of diffusion studies whose analysis benefits from the available computer capacity. These experiments provided information about the properties of Si vacancies at high temperatures. Similar studies are planned with Ge isotope multilayer structures. The self- and dopant diffusion experiments with isotopically enriched elemental and compound semiconductors yield information about the nature, charge states, transport capacities, and thermodynamic properties of atomic point defects. This shows that the study of atomic transport processes with isotope heterostructures provides similar information about point defects at high temperatures that spectroscopic methods do for low temperatures.

Diffusion experiments with isotope heterostructures can be also performed with any other material system for which enriched stable isotopes are available. Our present research interest concerns diffusion in Ge and SiGe alloys and the diffusion of the network components in silica and silicate glasses doped with alkali and alkaline-earth oxides.

Acknowledgements

We are grateful to many colleagues and collaborators for the numerous contributions to the

research reviewed here. Some of the reviewed work has been supported in part by the Director, Office of Science, Office of Basic Energy Sciences, Division of Materials Science and Engineering, of the U.S. Department of Energy under contract No. DE-AC03-76SF00098, in part by the Alexander von Humboldt Foundation and the Deutsche Forschungsgemeinschaft, and by U.S. NSF Grant No. DMR-0109844 and in part by a Max-Planck Society research prize.

References

1. H. Bracht, MRS Bulletin, 25 (2000) 22.
2. Landolt-Börnstein, New Series, Group III, Vol. 33a, Diffusion in Semiconductors (ed. D.L. Beke) (Springer, Berlin, 1998).
3. Landolt-Börnstein, New Series, Group III, Vol. 41a2α, Group IV Elements (ed. O. Madelung, U. Rössler, M. Schulz) (Springer, Berlin, 2002).
4. H.D. Fuchs, W. Walukiewicz, E.E. Haller, W. Dondl, R. Schorer, G. Abstreiter, A.I. Rudnev, A.V. Tikhomirov, V.I. Ozhogin, Phys. Rev. B 51 (1995) 16817.
5. M. Werner, H. Mehrer, H.D. Hochheimer, Phys. Rev. B 32 (1985) 3930.
6. N.A. Stolwijk, W. Frank, J. Hölzl, S.J. Pearton, E.E. Haller, J. Appl. Phys. 57 (1985) 5211.
7. H. Bracht, N.A. Stolwijk, H. Mehrer, Phys. Rev. B 43 (1991) 14465
8. H. Bracht, E.E. Haller, and R. Clark-Phelps, Phys. Rev. Lett. 81 (1998) 393.
9. H. Bracht, E.E. Haller, K. Eberl, M. Cardona, R. Clark-Phelps, Mater. Res. Soc. Symp. Proc. 527 (1998) 335.
10. H. Bracht, N.A. Stolwijk, and H. Mehrer, Phys. Rev. B 52 (1995) 16542.
11. A. Giese, H. Bracht, N.A. Stolwijk, J.T. Walton, J. Appl. Phys. 83 (1998) 8062.
12. A. Giese, H. Bracht, N.A. Stolwijk, D. Baither, Mater. Sci. Eng. B 71 (2000) 160.
13. A. Giese, doctoral thesis, University of Münster (2000).
14. L. Wang, L. Hsu, E.E. Haller, J.W. Erickson, A. Fischer, K. Eberl, M. Cardona, Phys. Rev. Lett. 76 (1996) 2342.
15. L. Wang, J.A. Wolk, L. Hsu, E.E. Haller, J.W. Erickson, M. Cardona, T. Ruf, J.P. Silveira, F. Briones, Appl. Phys. Lett. 70 (1997) 1831.
16. H. Bracht, E.E. Haller, K. Eberl, and M. Cardona, Appl. Phys. Lett. 74 (1999) 49.
17. H. Bracht, M. Norseng, E.E. Haller, K. Eberl, M. Cardona, Solid State Communications 112 (1999) 301.
18. G.A. Baraff, M. Schlüter, Phys. Rev. Lett. 55 (1985) 1327.
19. T.Y. Tan, U. Gösele, J. Appl. Phys. 52 (1988) 1240.
20. G. Bösker, N.A. Stolwijk, H. Mehrer, U. Södervall, J.V. Thordson, T.G. Anderson, A. Burchard, Mat. Res. Soc. Symp. Proc. 527 (1998) 347.
21. D. Weiler and H. Mehrer, Phil. Mag. A 49 (1984) 309.
22. H. Bracht, S.P. Nicols, W. Walukiewicz, J.P. Silveira, F. Briones, and E.E. Haller, Nature 408 (2000) 69.
23. H. Bracht, S.P. Nicols, E.E. Haller, J.P. Silveira, and F. Briones, J. Appl. Phys. 89 (2001) 5393.
24. S.P. Nicols, H. Bracht, M. Benamara, Z. Liliental-Weber, E.E. Haller, Physica B 308-310 (2001) 854.

25. J. Pöpping, N.A. Stolwijk, U. Södervall, Ch. Jäger, W. Jäger, Physica B 308-310 (2001) 895.
26. N.A. Stolwijk, J. Pöpping, Materials Science in Semiconductor Processing 6 (2003) 315.
27. H. Bracht, M.S. Norseng, E.E. Haller, K. Eberl, Physica B 308 (2001) 831.
28. H. Bracht, S. Brotzmann, submitted.
29. K. Rüschenschmidt, H. Bracht, N.A. Stolwijk, M. Laube, G. Pensl, G.R. Brandes, J. Appl. Phys. 96 (2004) 1458.
30. J.D. Hong, R.F. Davies, J. Am. Ceram. Soc. 63 (1980) 546.
31. J.D. Hong, R.F. Davies, D.E. Newbury, J. Mater. Sci. 16 (1981) 2485.
32. W. Shockley, and J.T. Last, Phys. Rev. 107 (1957) 392.
33. W.D. Laidig, N. Holonyak, Jr., M.D. Camras, K. Hess, J.J. Coleman, P.D. Dapkus, J. Bardeen, Appl. Phys. Lett 38 (1981) 776.
34. G. Bösker, N.A. Stolwijk, H.-G. Hettwer, A. Rucki, W. Jäger, U. Södervall, Phys. Rev. B 52 (1995) 11927.
35. I.D. Sharp H.A. Bracht, H.H. Silvestri, S.P. Nicols, J.W. Beeman, J. Hansen, A. Nylandsted Larsen, E.E. Haller, Mat. Res. Soc. Symp. Proc. 719 (2002) F13.11.1.
36. H. Bracht, H.H. Silvestri, I.D. Sharp, S.P. Nicols, J.W. Beeman, J.L. Hansen, A. Nylandsted Larsen, E.E. Haller, Inst. Phys. Conf. Ser. No 171 (2003) C3.8.
37. H.H Silvestri, I.D. Sharp, H. Bracht, S.P. Nicols, J.W. Beeman, J.L. Hansen, A. Nylandsted Larsen, E.E. Haller, Mat. Res. Soc. Symp. Proc. 719 (2002) F13.10.1.
38. H.H. Silvestri, Ph.D. thesis, University of California Berkeley (2004).
39. H.H. Silvestri, H.A. Bracht, I.D. Sharp, J. Hansen, A. Nylandsted-Larsen, and E.E. Haller, Mater. Res. Soc. Symp. Proc. 810 (2004) C3.3.
40. H. Bracht, J. Fage Pedersen, N. Zangenberg, A. Nylandsted Larsen, E.E. Haller, G. Lulli, M. Posselt, Phys. Rev. Lett. 91 (2003) 245502/1-4.
41. S. Uppal, A.F.W. Willoughby, J.M. Bonar, N.E.B. Cowern, T. Grasby, R.J.H. Morris, M.G. Dowsett, J. Appl. Phys. 96 (2004) 1376.
42. T. Takahashi, S. Fukatsu, K.M. Itoh, M. Uematsu, A. Fujiwara, H. Kageshima, Y. Takahashi, K. Shiraishi, J. Appl. Phys. 93 (2003) 3674.
43. S. Fukatsu, T. Takahashi, K.M. Itoh, M. Uematsu, A. Fujiwara, H. Kageshima, Y. Takahashi, K. Shiraishi, U.Gösele, Appl. Phys. Lett. 83 (2003) 3897.
44. M. Uematsu, H. Kageshima, Y. Takahashi, S. Fukatsu, K.I. Itoh, K. Shiraishi, U. Gösele, Appl. Phys. Lett. 84 (2004) 876.
45. H. Bracht, R. Staskunaite, E.E. Haller, P. Fielitz, G. Borchardt, D. Grambole, submitted.